

# Unexpected features of the formation of Si and Ge nanocrystals during annealing of implanted SiO<sub>2</sub> layers: Low frequency Raman spectroscopic characterization



Venu Mankad<sup>a</sup>, N.N. Ovsiyuk<sup>b</sup>, Sanjeev K. Gupta<sup>a</sup>, Prafulla K. Jha<sup>a,\*</sup>

<sup>a</sup> Department of Physics, Maharaja Krishnakumarsinhji Bhavnagar University, Bhavnagar 364001, India

<sup>b</sup> Institute for Geology and Mineralogy, Siberian Branch, Russian Academy of Sciences, Novosibirsk 630090, Russia

## ARTICLE INFO

### Article history:

Received 31 August 2013

Received in revised form

17 September 2013

Accepted 20 September 2013

Available online 27 September 2013

### Keywords:

Semiconductors

Ion-implantation

Raman-spectroscopy

Acoustical properties

## ABSTRACT

The present paper reports a study of the influence of heat treatments on the ion-beam synthesis of Si and Ge nanocrystals in SiO<sub>2</sub> layers by low-frequency Raman scattering. Low-frequency Raman scattering is used just because the appearance in the glass matrix of crystal nuclei leads to an additional contribution to the density of only low-frequency acoustic vibrational states due to surface vibration modes of the nuclei. Electron microscopy, contrary to expectations, revealed a decrease rather than increase in the size of the crystal nucleus during annealing. Additionally, low-frequency Raman spectra show that the samples do not have a smooth distribution of nanoparticle sizes, as expected, but two different sizes of Si and Ge nanocrystals. This similarity is surprising because Si and Ge have different diffusion coefficients, temperatures of crystallization, meltings, and binding energies. Despite this, in both cases the same mechanism operates during the growth of Si and Ge nanocrystals.

© 2013 Elsevier B.V. All rights reserved.

## 1. Introduction

Silicon and germanium nanocrystals embedded in a dielectric matrix have attracted great interest over the last few years for their important physical and chemical properties [1–12]. The main properties of these materials are related to the confinement of (quasi)particles (electrons, holes, phonons, excitons, etc.) in volume corresponding to the radii on the order of nanometers. A strong correlation between the particle size and the band gap has been established. For this reason, the essential requirement for different applications of Si and Ge nanoparticles is to have an accurate knowledge of the particle size, size distribution and particle growth. Simultaneous control of nanoparticles size and composition will extend the range of applications of nanoparticles/glass systems. In the past decade, there has been much interest in the vibrational properties of semiconductor nanoparticles as the emission of phonon is one of the most important electronic dephasing mechanisms. Particle sizes and surface structures have been shown to be the most important factors that decide optical properties and light emitting efficiencies of these nanostructure materials. Apart from modifying the electronic structure, the spatial confinement also alters the electron–phonon coupling, an important component to determine the Raman intensity. The acoustic phonon sidebands

encountered in the photoluminescence (PL) are found to affect energy relaxation in nanoparticles. The modification resulting into the phonon spectra mainly in the low frequency region from confinement resulted in a new field of nanoscale science, known as phonon engineering or nanophononics [13]. Reducing the size of electronic devices below the acoustic phonon mean free path gives new possibilities for phonon propagation and interaction. Raman scattering probes the vibrational states of the particles such as the confined acoustic, optical and surface phonon modes and provides an understanding of electron–phonon interactions. This has led to several investigations of acoustic vibrations of spherical nanoparticles, particularly the semiconductor nanoparticles leading to an understanding of the role of vibrations in the performance of some optical devices (for example, in electronic dephasing due to emission of phonons) [14,15]. Low-frequency Raman scattering caused by interaction of visible light with acoustic vibrational modes of nanocrystals has been used to study the particle size distribution and the coupling between the particle and matrix according to the vibrational theories of acoustic phonons confined in nanoparticles [16–22]. This is because of the fact that in nanoparticles due to violation of the wave vector conservation rule, the total density of vibrational states is observed in Raman scattering spectra. This feature allows one to study the initial stage of crystallization since the occurrence of crystal nuclei in a matrix of glass results in an additional contribution to density of the acoustic vibrational states associated with the surface vibrational modes of nanocrystals. More than 100 years ago, Lamb [16] discussed the

\* Corresponding author. Tel.: +91 278 2422650; fax: +91 278 2426706.  
E-mail addresses: [prafullaj@yahoo.com](mailto:prafullaj@yahoo.com), [pkj@bhavuni.edu](mailto:pkj@bhavuni.edu) (P.K. Jha).

vibrations of a homogenous spherical elastic body under stress-free boundary conditions. This provided sufficiently good agreement to confirm that confined acoustic phonon modes were really being observed. The nanoparticle vibrations can be classified by their angular momentum number  $l \geq 0$  and its  $z$  component  $m$  ( $m$ =azimuthal quantum number). The vibrational modes can be classified either as spheroidal or torsional. The torsional mode frequencies depend on the transverse acoustic phonon velocity  $v_t$ , while the spheroidal mode frequencies depend on both the longitudinal and transverse acoustic phonon velocity  $v_l$  and  $v_t$  respectively. The observation of these modes requires polarization measurements, since spherical vibrations lead to a polarized scattering, while the torsional vibrations bring about a depolarized scattering. It has been established [17] that only the lowest energy spheroidal modes with  $l$  equal to 0 and 2 are Raman active. The glass matrix influences the eigen-frequencies of the surface vibrational modes of nanocrystals [18]. To understand the crystallization of nanoparticles in glass matrix, modified models based on Lamb's theory such as complex frequency [12,14,19–22] and core-shell models [12,20–23] can be used which are quite successful in the interpretation of acoustic modes of nanoparticles embedded in medium.

In the present paper, we present an analysis of the formation of the most important group IV semiconductor nanocrystals such as Si and Ge glass matrix which has attracted much interest because of their potential applications in Si based optoelectronics, nanophotonics and electronic/optical memory devices. Further, interest to study the low frequency Raman scattering in these two semiconductors is due to the fact that the Ge nanocrystals show stronger confinement effect [23] resulting from direct gap semiconductor nature [24] in contrast to Si nanocrystals. This may be useful in understanding the formation of two different types of nanocrystals in different hosts. Out of several techniques to form nanocrystals of Si and Ge like doping of nanocrystals [25,26], use of pulsed heat treatments [27], introduction of additional precipitation centers [28,29], etc., the ion implantation technique is another possible method for the formation of nanocrystals. However, there is a requirement of intermediate heat treatments to form nanocrystals using ion implantation and in clarifying the mechanism of their formation [30–33]. It will be seen in what follows that the same mechanism operates even during the growth of Si and Ge nanocrystals.

## 2. Samples and experimental details

Silicon and germanium nanocrystals are prepared using implantation of  $\text{Si}^+$  and  $\text{Ge}^+$  ions at room temperature on  $\text{SiO}_2$  films of  $0.6 \mu\text{m}$  thickness with the dose of  $\sim 10^{17} \text{ cm}^{-2}$  [30] and energy in the range of 140–150 keV. It has been found that Si and Ge clusters are formed immediately after implantation.  $\text{Si}^+$  implanted  $\text{SiO}_2$  layers have been heat treated at  $1100^\circ\text{C}$ . However, the annealing has been carried out within 30 min for Si NCs. Evolution of Si and Ge NCs has been studied using low frequency Raman scattering and optical Raman spectra. Some preliminary results are presented elsewhere [33]. Raman spectra were recorded at room temperature in the backscattering geometry with vertically polarized  $532 \text{ nm}$  laser. Scattered light from the samples is dispersed using a double monochromator (Spex, model 14018) and detected using a photomultiplier tube ITT FW-130 operating in the photon-counting mode. Scanning of the spectra and data acquisition was carried out using a microprocessor based data-acquisition-cum-control system. Low frequency Raman spectra have been recorded from  $5$  to  $50 \text{ cm}^{-1}$  at steps of  $0.5 \text{ cm}^{-1}$  while optical Raman spectra were recorded in the range of  $40$ – $1500 \text{ cm}^{-1}$  using the same Raman spectrometer. Raman scattering experiments have been carried out on the samples

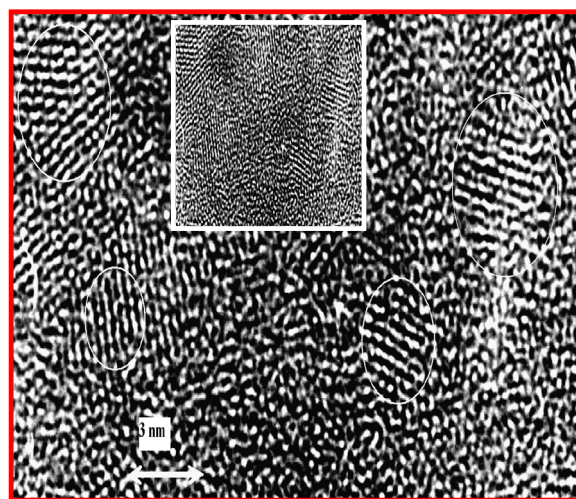


**Fig. 1.** Images of transverse sections of the sample after annealing at  $1100^\circ\text{C}$  for Si nanoparticles. Lattice fringes corresponding to the  $\{111\}$  planes of Si can be clearly seen which are encircled. Two nanocrystals with a diameter of about  $3 \text{ nm}$  and  $6 \text{ nm}$  are shown.

placed in vacuum to eliminate air lines during recording of the low frequency spectra. The spectra have been recorded several times under the same conditions and data have been accumulated in order to detect less intense lines and to improve the signal to noise ratio. In order to fit the measured Raman spectra first the exponential background is subtracted from the observed data to remove the Rayleigh background in Figs. 2 and 3. This is followed by a straight line subtraction for the appearance of modes. After subtraction, the resulting spectrum is deconvoluted by Lorentzian contours using a peak fit process, i.e., by PEAKFIT software. The correctness of the process is confirmed by the final fitted spectrum (full curve in figure) passing through the observed data and most importantly is the resultant of the addition of all peaks under the fitted curve. The morphology of the NCs was characterized by a high resolution electron microscope (Fig. 1).

## 3. Results and discussion

Experiments were conducted to study the structure of nanocrystals with high-resolution transmission electron microscopy. Fig. 1 shows a typical electron micrograph of Si nanocrystals embedded in a  $\text{SiO}_2$  matrix. We can clearly see lattice fringes corresponding to the  $\{111\}$  planes of Si nanocrystals. According to electron diffraction, the interlayer distance is  $0.314 \text{ nm}$ , which corresponds to silicon, while for germanium this distance is greater and equal to  $0.327 \text{ nm}$ . It is found that each Si nanocrystal is a single crystal with good crystallinity and they are well dispersed in  $\text{SiO}_2$  matrices. From this micrograph, we can observe two average sizes of Si nanocrystals of  $3 \text{ nm}$  and  $6 \text{ nm}$ . A TEM micrograph where only Si NPs with single sized particle is observed, a figure of interest, is shown in Fig. 1 of Ref. [33]. Figs. 2 and 3 respectively depict the low frequency Raman spectrum of Si and Ge NCs embedded in  $\text{SiO}_2$ . Both spectra show the presence of two peaks which are caused by the interaction of visible light with the acoustic vibrational modes of nanocrystals. These two peaks which correspond to the particle of two different sizes are due to the spheroidal mode with angular momentum  $l=0$  and index  $n=0$  (symmetric mode) as the peaks are recorded with polarized scattering. In the case of polarized Raman scattering the field vector of the exciting and scattered waves is parallel to the scattering plane, while the other Raman active spheroidal mode  $l=2$  (quadrupolar mode) provides depolarized spectra. Fig. 2(a) shows that the two peaks due to spheroidal

Download English Version:

<https://daneshyari.com/en/article/1810011>

Download Persian Version:

<https://daneshyari.com/article/1810011>

[Daneshyari.com](https://daneshyari.com)